Sonic Fatigue of Advanced Composite Panels in Thermal Environments

M. J. Jacobson*
Northrop Corporation, Hawthorne, California

Combined analytic and experimental activities were performed to evaluate an advanced structural design concept for advanced composite fuselage panels suitable for V/STOL aircraft. An existing sonic fatigue analysis procedure was then evaluated. Both flat and slightly curved multibay cross-stiffened panels with graphite-epoxy skins were designed, analyzed, fabricated, and tested. The panels simulated skin-frame-stringer aircraft structure. The joints of the substructure and skin were achieved in a single-cure autoclave operation without an adhesive. The substructure consisted of graphite-epoxy hat-section stringers and glass-epoxy J-section frames. Some panels were tested in a combined acoustic-thermal environment, and others were tested in an acoustic environment at room temperature. The sonic fatigue tests were performed in a progressive wave acoustic test chamber with broadband excitation at approximately 163.5-dB overall sound pressure level. The sonic fatigue lives of the test panels exceeded the predicted lives obtained with existing semiempirical methods developed for graphite-epoxy and aluminum alloy panels featuring other design concepts and manufacturing processes.

Introduction

IN certain operational modes of projected V/STOL aircraft, combined thermal and acoustic environments may occur in some area of the fuselage, wing, and empennage structure—the locations and magnitudes being highly dependent on the vehicle/engine configuration. Noise sources include engine air intake duct turbulence, jet engine exhaust, and high-speed flight during which the aircraft skin is acted upon by boundary-layer noise and high temperatures induced by aerodynamic heating. Furthermore, of particular importance are noise reflections, heat flow, and airflow during liftoff from ship decks or ground surfaces which may significantly increase the intensities of the acoustic and thermal environments to which portions of V/STOL aircraft structure may be subjected. Thus, the design of the aircraft structural panels which may experience service in combined acoustic-thermal environments is important to a variety of projected V/STOL aircraft.

Thin-skinned, integrally stiffened advanced composite structure is under consideration for application in the fuselage and other portions of V/STOL aircraft. Many regions of such structure may be mildly curved or flat, and are therefore considered especially prone to fatigue failures in high-intensity sonic environments. Consequently, there are concerns that sonic fatigue will govern the design of these advanced composite structures.

Previously, several government sponsored programs[1-5] were conducted to develop sonic fatigue design methods and supporting test data for metallic structure in room temperature (RT) environments. In addition, programs[6-8] were then conducted in which composite structural materials were used instead of metals, and elevated temperature environments for metallic structures were considered.[9,10] As a result, considerable sonic fatigue design methodology,[11] principally based on semiempirical approaches, has been developed, and certain types of sonic fatigue failures have diminished in number or been eliminated.

The objective of the activity[12] that is the subject of this paper was to evaluate representative design concepts and sonic fatigue analysis procedures for advanced composite fuselage panels suitable for application to V/STOL aircraft exposed to combined acoustic-thermal environments in service. This activity consisted of a combined theoretical and experimental effort involving material selection; design, analysis, and fabrication of stiffened graphite-epoxy acoustic test panels simulating fuselage panels; and acoustic testing with some tests conducted in a combined acoustic-thermal environment, i.e., at a high sound pressure level (SPL) and elevated temperature, and the remainder at a high SPL at room temperature.

Presented as Paper 81-1699 at the AIAA Aircraft Systems and Technology Conference, Dayton, Ohio, Aug. 11-13, 1981; submitted Sept. 23, 1981; revision received June 1, 1982.

*Senior Technical Specialist. Member AIAA.

Specimen Design and Manufacture

The design of the test specimens was chosen to be compatible with expected flight vehicle requirements for fuselage panels suitable for application to V/STOL aircraft. The manufacturing approach featured a single-cure process in an autoclave operation in which the panel skin and substructure were cured and joined together without an adhesive. In all, eight panels were designed, manufactured, and subjected to acoustic tests.

Key features of the panels and the test conditions are summarized in Table 1. Additional detailed information on the panel designs and manufacturing procedures is documented elsewhere.[12] The panels contained skins with either five plies and a $[\pm 45/90]_s$ layup or nine plies and a $[(\pm 45)_2/90]_s$ layup, with the 90-deg direction perpendicular to the hat-section stringers. The overall panel size was 36×23 in., which allowed the sonic fatigue tests to be conducted in the 48×48-in. test section of Northrop's progressive wave acoustic test chamber (Fig. 1). The overall sound pressure levels (OASPLs) in the tests were 163.5 ± 0.5 dB, with some panels experiencing slightly more than 163.5 dB and others slightly less.

Both curved and flat panels were included in the test program. A 100-in. radius of curvature was selected as representative of curved side fuselage panels. Flat panels were selected to obtain baseline data.

All of the eight test panels featured AS/3501-6 graphite-epoxy skin, graphite-epoxy hat-section substructure simulating stringers, and HMF 1581/3501-6 glass-epoxy J-section substructure simulating fuselage frames. Unidirectional AS/3501-6 graphite-epoxy tape of 0.005 in. thickness and HMF 1581/3501-6 glass-epoxy cloth were used in the manufacture of the panels.

The design of panels N-2 (Fig. 2) and N-3 was identical in all features except one; namely, in panel N-2 the hat-section substructure was stitched[12] to the skin (Fig. 3), whereas there was no stitching in panel N-3. In the case of identical panels

Table 1 Summary of test conditions and panel descriptions

Test no.	Panel designation	Stitching	Radius of curvature, in.	Number of stringers	Number of skin plies	Stringer spacing, in.	Frame spacing, in.	Overall sound pressure level, dB	Target temperature, F
1	N-1	No	100	3	5	7	24	164	250
2	N-3	No	∞	2	9	12	24	164	RT
3	N-2	Yes	∞	2	9	12	24	163	RT
4	A-1	No	100	2	9	12	24	163	250
5	AA-1	No	100	2	5	12	24	164	250
6	AA-2	No	100	2	5	12	24	164	RT
7	AA-5	No	∞	2	5	12	24	163	250
8	AA-6	No	∞	2	5	12	24	163	RT

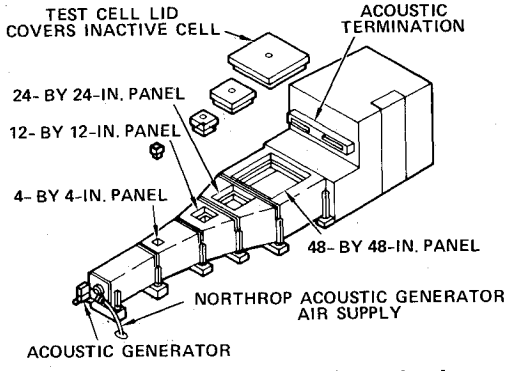

Fig. 1 Progressive wave acoustic test chamber.

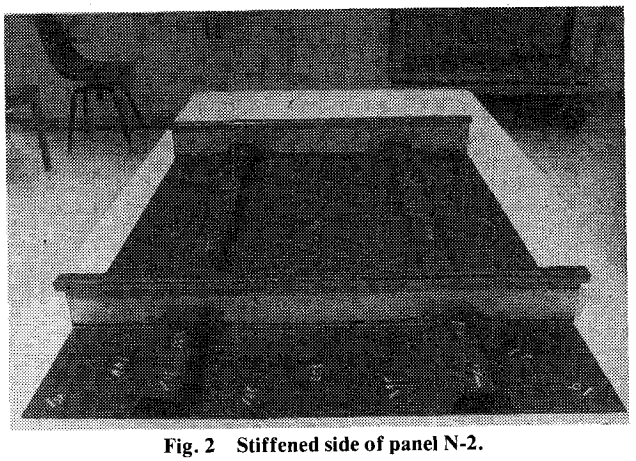

Fig. 2 Stiffened side of panel N-2.

(i.e., the AA-1 and AA-2 pair and the AA-5 and AA-6 pair), the sonic fatigue test of one panel was conducted at room temperature and the sonic fatigue test of the other was conducted at elevated temperature to determine the effect of temperature.

Test Conditions and Procedures

For one configuration of a horizontal attitude V/STOL aircraft that was under investigation at the beginning of the activity reported in this paper, vertical thrust is obtained from the afterburning turbojets, which exhaust directly downward; the aircraft is thus subjected to heat and noise reflected from the ship deck. An analytic study of the sonic environment to which the fuselage panels of this V/STOL aircraft are subjected during liftoff and landing resulted in predictions of at least 153-167-dB OASPL for the side and bottom fuselage skins at liftoff, decreasing approximately 7 dB at an altitude of one wing semispan. From other studies it was concluded that critical lightweight fuselage panels may operate during liftoff and landing in high-intensity sonic environments at temperatures in the vicinity of 250 F.

In addition, it was concluded that for that particular aircraft configuration, the backside (i.e., inside the aircraft) of fuselage panels relatively close to the fuselage-mounted engines would be hotter than the front side (i.e., outside the aircraft), whereas the front side of the panels would be hotter for panels farther from the engines. Furthermore, it was anticipated that backside heating may result in a more severe thermal-acoustic environment than front-side heating for certain combinations of temperature, SPL, panel curvature, and other design features. For these reasons, and because backside heating of the panels with hot air was easier to achieve experimentally than front-side heating, it was decided to use backside heating in the test program.[12]

All of the sonic fatigue tests were conducted at approximately 163.5-dB OASPL irrespective of test temperature. A target temperature of 250 F was established for the sonic fatigue tests at elevated temperature. There were differences in experimental temperature not only between the substructure and skin but also through the thickness and on each skin surface. Skin temperatures generally ranged from approximately 200 to 250 F. The heating in the tests was controlled so that no measured temperature would exceed 300 F as a safeguard against extreme matrix degradation in the fiber-epoxy systems.

For modal survey and sonic fatigue tests, each of the test panels was attached at its boundary to a test fixture (Fig. 4) in the form of a box frame approximately the size of the test panel and 5 in. deep. One flat and one curved test fixture sufficed for all the tests. Angle clips were used to attach the ends of the substructure to the test fixture, which was attached to a 48×48-in. jig plate that closed off the test cell during progressive wave test chamber testing. The test panel was located such that it effectively became a portion of the upper wall of the chamber during the tests in the acoustic chamber.

Each test panel was strain-gaged, and those panels that were to experience elevated temperature tests were instrumented with thermocouples. Each test panel was instrumented with at least six strain gages on the unstiffened side of the central bay (Fig. 5). Strain gages 1 and 2 were installed parallel and perpendicular, respectively, to the acoustic flow direction, and strain gages 3-6 were centered over the outer edge of the flange of the substructure in the central bay. At least ten thermocouples were installed on the skin and substructure of all panels subjected to elevated temperature tests.[12]

The substructure and joints bounding the central bay, as well as the central bay itself, were the test sections of interest in the sonic fatigue tests. The peripheral bays, as well as the substructure and joints separating the peripheral bays, were considered to be a part of the test fixture, in the sense that any structural failures occurring in the outer bays were not considered as legitimate failures for the purpose of determining the sonic fatigue life of a test panel. Thus, whenever structural degradation was observed in the skin, substructure, or joint of an outer bay, the sonic fatigue test was suspended

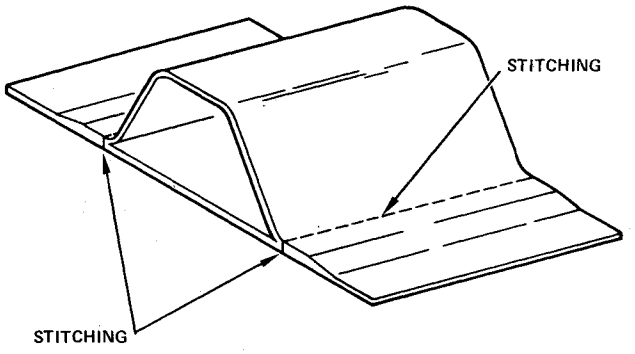

Fig. 3 Schematic of stitching location on hat-section stiffener and skin.

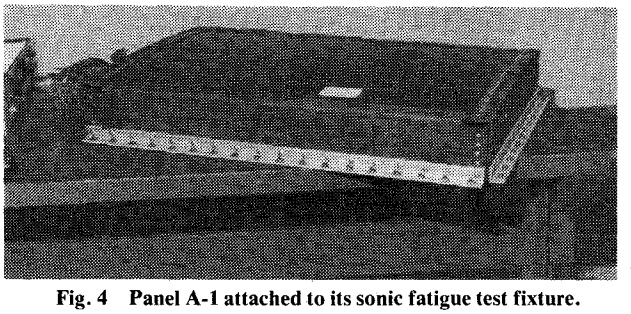

Fig. 4 Panel A-1 attached to its sonic fatigue test fixture.

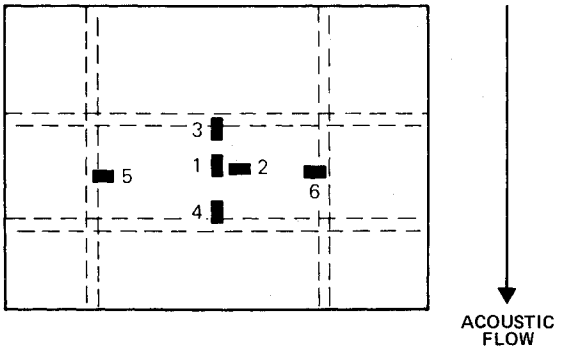

Fig. 5 Schematic of strain gage locations in central bay of test panels.

in order to determine whether to repair the outer bay damage and continue the sonic fatigue test or to terminate the test and state that a runout time had been achieved for the test panel.

After the panels were instrumented with strain gages and thermocouples, they were subjected to loudspeaker excitation tests to obtain natural frequencies, modal shapes, and damping data.[12] The panels to be tested in acoustic-thermal environments were subjected to heating at ambient SPL to determine the spatial variation of temperature. All panels were then subjected to tests at the elevated temperature of the sonic fatigue test. In the tests, the OASPL was raised from 136 to 160 dB in increments of 6 dB, and strain-pressure-temperature measurements were recorded at each OASPL. The OASPL was then raised to approximately 163.5 dB, the strain-temperature-pressure data were recorded, and a long-duration sonic fatigue test was initiated to determine the fatigue life and failure mode of the panel.

During the acoustic tests, not only were on-line strains observed, but strain signals were taped and used in determining the average strain from the signals and the rms value of the alternating component of strain. Experimental pressures were also recorded. A typical one-third-octave-band plot of the acoustic pressure and a narrow-band plot of the

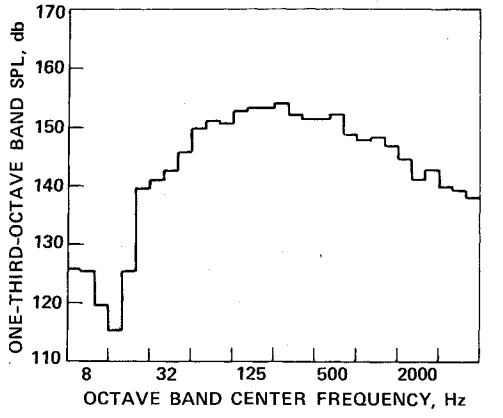

Fig. 6 One-third-octave-band SPL of panel A-1 at 163-dB OASPL.

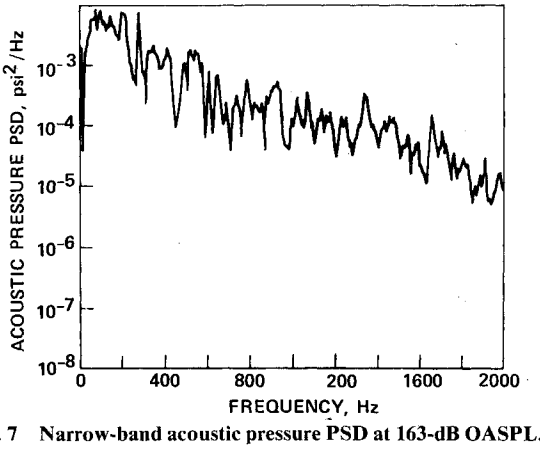

Fig. 7 Narrow-band acoustic pressure PSD at 163-dB OASPL.

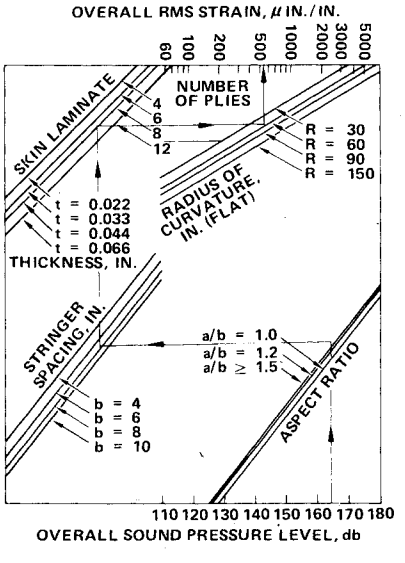

Fig. 8 Root-mean-square strain nomograph (from Ref. 8).

acoustic pressure power spectral density (PSD) during a test at 163-dB OASPL are presented in Figs. 6 and 7. Key instruments used in the tests were a B&K 2607 measuring amplifier for rms values of alternating strain, a Fluke 8120 dc digital voltmeter for average strain, a Sangamo Saber II FM tape recorder for strain gage and microphone signals, a Nicolet 444 Fourier analyzer for one-third-octave-band and narrow-band spectral analyses, a Kaye Ramp data logging system for temperature data, copper-constantan thermocouples, and WK-06-250BG-350 temperature-compensated strain gages.

Modes of Sonic Fatigue Failure

Four of the eight test panels (namely, panels AA-1, AA-2, AA-5, and N-3) experienced sonic fatigue failures either in their central bays or the joints or substructure surrounding the central bay (Table 2). Photographs of the failures were taken for documentation.[12] The failures were of sufficient severity that repairs would have to be performed if the damage had been detected on actual aircraft in service.

At the initiation of the test activity, 50-80 h was established as the runout time at which a sonic fatigue test would be suspended if a failure was not detected in a panel's central bay or one of its surrounding joints or substructural elements. Panel AA-6 achieved the target runout time and its test was then terminated. In the test of panel N-3, a graphite fiber popped through the unstiffened side of the skin opposite a hat-section joint in the central bay between 31 and 37 h of acoustic exposure. However, the damage did not propagate, and the planned runout time of 50 h was achieved.

The sonic fatigue test of panel N-1 was suspended at 3.5 h of acoustic exposure and the test of panel N-2 at 13.5 h of exposure because of substructure damage attributed to the joints between the substructure and the test fixture. It was decided not to repair the damage in the peripheral bays of these two panels; the time at which the N-1 and N-2 panel tests were suspended thus became the runout time.

From Table 2 it is observed that in the sonic fatigue tests of the two pairs of identical panels (panels AA-1 vs AA-2 and AA-5 vs AA-6) with one member of the pair tested at elevated temperature with backside heating and the other member tested at room temperature, the sonic fatigue life was less in the elevated temperature test. The modes of failure (see Table 2) were dependent on the temperature.

Evaluation of an Existing Sonic Fatigue Analysis Methodology

A semiempirical methodology[8] was recently developed for predicting the sonic fatigue life of graphite-epoxy panels. The strain-vs-acoustic pressure nomograph and random *S-N* curve from Ref. 8 are reproduced here as Figs. 8 and 9, respectively.

The methodology of Ref. 8 was applied to predict the sonic fatigue lives of the current test panels (Table 3). This methodology was developed for panels with Z- and J-section stiffeners and used for the panels with hat-section stringers (Table 1); consequently, some disagreement was expected between the experimental frequencies, strain response, and sonic fatigue life generated in this program and the values predicted using Ref. 8 methodology.

The sonic fatigue analysis methodology that was used consists of a three-step process. In the first step, a nomograph

Table 2 Summary of sonic fatigue test results at 163- and 164-dB OASPL

Panel designation	Number of skin plies	Radius of curvature, in.	Stringer spacing on centers, in.	Stitching	Elevated temperature test	Life, h	Mode of failure
A-1	9	100	12	No	Yes	>56	...
AA-1	5	100	12	No	Yes	7-14	Joint of J section to skin and also skin failure
AA-2	5	100	12	No	No	17-19.5	Massive failure in skin in a quadrant of center bay
AA-5	5	∞	12	No	Yes	15-17	J section frame failure
AA-6	5	∞	12	No	No	>84	...
N-1	5	100	7	No	Yes	>3.5	...
N-2	9	∞	12	Yes	No	>13.5	...
N-3	9	∞	12	No	No	>50	...

Table 3 Comparisons of predicted and experimental rms strain, frequency, cycles to failure, and time to failure

Panel designation	Stringer spacing, in.	rms strain		Frequency		Fatigue life		Fatigue life	
		Theoretical, μin./in.	Experimental, μin./in.	Theoretical, Hz	Experimental, Hz	Theoretical, 10^5 cycles	Experimental, 10^5 cycles	Theoretical, h	Experimental, h
N-2	9.75	695	489	121	160	4.0	>75	0.9	>13
N-2	12.00	875	489	83	160	<1.5	>75	<0.5	>13
N-3	9.75	695	466	121	165	4.0	>300	0.9	>50
N-3	12.00	875	466	83	165	<1.5	>300	<0.5	>50
A-1	9.75	555	542	261	170	17.0	>340	1.9	>56
A-1	12.00	699	542	243	170	3.6	>340	0.4	>56
AA-1	9.75	1127	700	257	202	<1.5	96	<0.2	7-14
AA-1	12.00	1418	700	201	202	<1.5	96	<0.2	7-14
AA-2	9.75	1127	400	257	45	<1.5	1100	<0.2	17-19
AA-2	12.00	1418	400	201	45	<1.5	1100	<0.2	17-19
AA-5	9.75	1764	450	74	198	<1.5	210	<0.6	15-17
AA-5	12.00	2224	450	49	198	<1.5	210	<0.9	15-17
AA-6	9.75	1764	420	74	194	<1.5	>1200	<0.6	>84
AA-6	12.00	2224	420	49	194	<1.5	>1200	<0.9	>84
N-1	4.75	508	...	398	...	35.0	...	2.4	>3.5
N-1	7.00	783	...	292	...	1.8	...	0.2	>3.5

(Fig. 8) is used to predict the overall rms strain response expected to govern the sonic fatigue life of a rectangular panel. The strain is a function of OASPL, stringer spacing, aspect ratio of a bay of the multibay panel, number of plies (i.e., panel thickness), and radius of curvature, with the stringers assumed to be in the straight direction of the panel. The predicted rms strain response is in the skin at a joint with the stringer and midway between the fuselage frame members. In the second step, a chart (not presented in this paper) is used to predict the unstiffened panel's fundamental frequency under the assumption that the panel is fully fixed on all four edges. In the third step, a random *S-N* curve (Fig. 9) is used to predict cycles to failure on the basis of overall rms strain obtained in the first step. The time to failure is then computed as the quotient of the cycles to failure obtained in step 3 divided by the response frequency obtained in step 2.

No modifications were made to the equations, nomographs, and charts that comprise the methodology when it was applied to obtain the predictions of overall rms strain, fundamental frequency, and number of cycles to failure presented in Table 3. Calculations were made for two stringer spacings: the first was equal to the distance between the centerlines of the two stringers and the other was equal to the distance between the edges of stringer flanges in the central bay of the test panels.

Table 3 also contains experimental strains, predominant response frequencies, and cycles to failure for correlation with the predictions. Only the larger of the experimental strains at the center of the two long sides in the central bay is reported in Table 3. In general, the larger of the two strains was nearly equal to the smaller strain. However, in the test of panel A-1, the experimental strains at the center of the two long sides in the central bay were 542 and 240 μin./in.

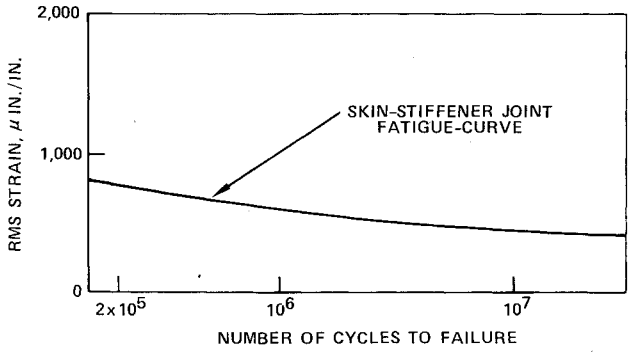

Fig. 9 Random fatigue curve for bonded skin-stiffener joint (from Ref. 8): rms strain vs cycles to failure.

The experimental number of cycles to failure in Table 3 was computed as the product of the experimental predominant response frequency and the experimental time to failure. For panel AA-1, the experimental life was computed using a frequency of 202 Hz for 7 h. For panel AA-2, the experimental life was computed using a frequency of 45 Hz for 17 h. For panel AA-5, the experimental life was computed using a frequency of 198 Hz for 15 h. For panel AA-6 the runout number of cycles (1.2×10^8 cycles) was computed using a frequency of 194 Hz for 84 h.

The predicted overall strains generally exceeded the experimental overall rms strains by a large margin (see Table 3). It was therefore expected (and subsequently verified) that the experimental sonic fatigue lives would exceed the predicted sonic fatigue lives. Other items of interest are presented in the following discussion.

From Fig. 9, one would expect that panel AA-6, which was flat and tested at room temperature, would have experienced a 56% greater strain response than panel AA-2, which was curved and tested at room temperature; however, the experimental rms strains (Table 3) in the skin at the center of the stringers of panels AA-2 and AA-6 were essentially the same (approximately 425 μin./in.). Furthermore, from Table 3, which lists experimental rms strain at both the center and the edge of the test panel central bay, it is observed that panel AA-2, which is curved, experienced a much greater rms strain than panel AA-6 (i.e., 950 μin./in. vs 310 μin./in.). It is believed that panel AA-2 was experiencing dynamic snap-throughs that were manifested by the extremely large strains at the panel center and greater strains in the skin at the stringers than had been expected. Dynamic snap-throughs are defined as occurring when a panel intermittently snaps from one curved equilibrium position to another in the high-intensity acoustic environment, at room temperature or elevated temperature.

The experimental rms strain in panels N-2 and N-3, with nine-ply flat skins, is greater than the rms strain of panel AA-6, with a five-ply flat skin (Table 4). This is contrary to the predictions of Table 3 and may be due to greater membrane strains in the thinner panel.

It is also noteworthy that the experimental fundamental frequency of panel N-1 obtained under loudspeaker excitation was an overall panel mode (at 178 Hz), whereas its predicted fundamental frequency (at least 292 Hz from Table 3) was obtained under the assumption that the central bays of panel N-1 were clamped at the edges. The implication is that sufficiently close spacing of the stringers results in an overall panel mode as the fundamental mode of the panel.

The random *S-N* curve (Fig. 9) was applied to predict the cycles to failure on the basis of known experimental rms strains. Table 4 contains experimental overall rms strains, the

Table 4 Evaluation of *S-N* curve of Fig. 9

Panel designation	rms test strains: Panel center, μin./in.	rms test strains: Panel joint, μin./in.	Predicted cycles to failure: Panel center, cycles	Predicted cycles to failure: Panel joint, cycles	Experimental data: Lower bound on panel life, h	Experimental data: Upper bound on panel life, h	Experimental data: Lower bound on cycles to failure of test panel, cycles	Experimental data: Upper bound on cycles to failure of test panel, cycles
A-1	796	537	1.3×10^5	2.5×10^6	56	?	3.4×10^7	?
AA-1	740	700	2.7×10^5	3.5×10^5	7	14	5.1×10^6	1.0×10^7
AA-2	950	420	$<1.3\times10^5$	1.8×10^7	17	19.5	2.7×10^6	3.2×10^6
AA-5	300	450	$>3.0\times10^7$	8.5×10^6	15	17	1.0×10^7	1.2×10^7
AA-6	310	430	$>3.0\times10^7$	1.6×10^7	84	?	5.8×10^7	?
N-1	...	...	...	...	...	...	...	...
N-2	411	489	2.0×10^7	5.0×10^6	13	?	7.5×10^6	?
N-3	450[a]	466	8.5×10^6	6.2×10^6	31	?	1.8×10^7	?

[a] Estimated strain.

predicted cycles to failure obtained from Fig. 9 in combination with the known overall rms strains, and upper and lower bounds on the experimental sonic fatigue life. The experimental cycles to failure were computed as the product of time to failure (from Table 4) and experimental frequency (from Table 3). The conclusion reached after an examination of Table 4 was that the application of the *S-N* curve of Fig. 9 was conservative inasmuch as the experimental lives exceeded predicted lives.

The differences between experimental frequencies, strain response, and sonic fatigue life generated in this program and the values predicted from the methodology reported in Ref. 8 are attributed principally to the following:

1) The methodology was developed for panels with Z- and J-section stiffeners and was used in this program for panels with hat-section stringers.

2) Layup sequence of composite structure is not accounted for in the sonic fatigue *S-N* curve (Fig. 9).

3) The assumption that sonic fatigue life is governed principally by the structural response in a panel's fundamental mode may not be appropriate.

4) Average strains, that were larger relative to alternating strain peaks in elevated temperature tests than in room temperature tests, were neglected in predictions of rms strain and life. However, even during the elevated temperature tests at approximately 163.5-dB OASPL, the rms value of the alternating strains exceeded the average strain at each strain gage in the central bay, thereby implying that the sonic fatigue failures could be attributed principally to the alternating strains. The thermally induced average strains in elevated temperature tests were due to temperature gradients and differences in the coefficients of thermal expansion of the panel skin, panel substructure, and test fixture.

5) Dynamic snap-throughs are not accounted for in predictions of strain response (Fig. 8) and life (Fig. 9).

6) Elevated temperature effects on the material properties were not accounted for because their effects were considered to be of secondary importance in this program.

Sonic Fatigue Resistance of Bonded Aluminum Panels vs Single-Cured Composite Panels

In a report on a sonic fatigue research program concerned with bonded multibay aluminum alloy panels for aircraft application,[5] it was concluded that the sonic fatigue resistance of the bonded aluminum panels was greater than riveted multibay aluminum alloy panels of comparable size and skin thickness. The bonded aluminum test panels were referred to as primary aluminum bonding structural technology (PABST) panels.

The PABST panels consisted of 7075-T6 aluminum alloy skins bonded to deep I-section and shallow J-section substructure simulating fuselage frames and longerons, respectively. A comparison of *S-N* data from the test of panel N-3 and the tests of the PABST panels A-4-1 and A-4-2 has been performed. Panels N-3, A-4-1, and A-4-2 all have the same nominal dimensions of the central bay; namely, 24 by 12 by 0.05 in.

The PABST panels A-4-1 and A-4-2 experienced sonic fatigue failures at 5 h of acoustic exposure at 166-dB OASPL with a predominant and fundamental response frequency of 140 Hz. The sonic fatigue life was computed as the product of the predominant frequency and the time to failure. The life was 2.5×10^6 cycles. Based on the slope of the sonic fatigue curve in Ref. 5, the sonic fatigue life of the PABST panels was estimated to increase by 67% for a 2.5-dB drop in OASPL (this increase did not account for a small change in response frequency because of the 2.5-dB drop). It is thus predicted that panels A-4-1 and A-4-2 would have achieved a life of 4.2×10^6 cycles at 163.5-dB OASPL.

The graphite fiber pop-through of panel N-3 is assumed to have occurred at 34 h of exposure, which was approximately midway between the last inspection without an observation of the surface crack and the first inspection when the surface crack was observed. The predominant and fundamental frequency of panel N-3 during the sonic fatigue test was 160 Hz, and the computed time to the fatigue-induced damage of panel N-3 was thus 19.6×10^6 cycles.

The time to the first sonic fatigue damage of composite panel N-3 is thus 19.6/4.2, or 4.7 times the predicted life of the PABST panels with the same nominal central bay dimensions, thereby implying that panel N-3 is more sonic fatigue resistant than the PABST panels. However, the acoustic flow in the PABST panel tests was along the length direction of the panels' central bay, whereas the acoustic flow in the test of panel N-3 was along the width direction. The exact effect of the acoustic flow direction on sonic fatigue life is unknown; however, the effect is not believed to be large enough to alter the conclusion that the graphite-epoxy panels typified by panel N-3 are more sonic fatigue resistant than the aluminum-bonded PABST panels typified by panels A-4-1 and A-4-2.

Damping Factors

An examination of the experimental damping factors obtained with the logarithmic decay method in the test program was performed to determine the applicability of the damping factor in the sonic fatigue analysis methodology.

The damping factors in the fundamental mode of panels N-1, N-3, A-1, AA-1, AA-2, AA-5, and AA-6 ranged from 0.014 to 0.042, and their average value was 0.025, which is approximately twice the value reported for riveted aluminum alloy panels[3] and bonded aluminum alloy panels.[5] Damping factors averaging approximately 0.017 were obtained for bonded advanced composite panels.[7] Damping factors ranging from 0.02 to 0.08 for bonded composite panels were reported, but typically were from 0.02 to 0.03.[8]

Because of the considerable scatter in damping in the testing performed in Ref. 8 and the fact that the damping did not show any significant correlation with the strain data, damping was excluded as a design parameter in the semiempirical methodology developed in Ref. 8. This exclusion appears warranted based on the data reported both in this test program and in Ref. 8.

Conclusions

The multibay composite panel design concept featuring hat-section stringers, J-section frames, and a single-cure manufacturing process without an adhesive resulted in graphite-epoxy panels with excellent sonic fatigue resistance. The sonic fatigue lives of the graphite-epoxy test panels exceeded the predicted sonic fatigue lives of bonded aluminum alloy panels, riveted aluminum alloy panels, and bonded graphite-epoxy panels of comparable bay dimensions and skin thickness.

Use of the acoustic strain response nomograph and the sonic fatigue *S-N* curve from Ref. 8 resulted in unconservative estimates of strain response and conservative estimates of sonic fatigue life of the eight test panels reviewed in this paper.

The state of the art for predicting sonic fatigue life, acoustic strain response, and natural frequencies of multibay curved and flat composite panels subjected to high-intensity acoustic excitation at elevated temperature and room temperature needs improvement to render the methodology more useful for design purposes. There is also a need for verified methodology for predicting dynamic snap-throughs in acoustic environments and the effects of the snap-throughs on sonic fatigue life.

In the sonic fatigue tests of two pairs of identical panels with one member of the pair tested at elevated temperature with backside heating and the other member tested at room temperature, the sonic fatigue life was less in the elevated

temperature test. Elevated temperature test results with front-side heating would be useful, but even in their absence it is evident that sonic fatigue may be the controlling design factor for V/STOL composite fuselage panels in high-intensity acoustic environments characterized by certain combinations of sound pressure levels, temperatures, and thin-skinned curved and flat multibay structure. The sound pressure levels and temperatures in service are very dependent on the vehicle/engine configuration.

In subsequent tests to develop and verify further the sonic fatigue methodology addressed in this paper, it will be desirable to provide back-to-back strain gages to obtain membrane and bending data.

Acknowledgment

Activity reported in this paper was performed under Contract N62269-80-C-0240 for the Naval Air Development Center with J. Minecci, Program Manager, and R. Vining, Project Engineer.

References

[1] "Structural Design for Acoustic Fatigue," Aeronautical Systems Division, ASD-TDR-63-820, Oct. 1963.

[2] Jacobson, M.J. et al., "Honeycomb Structure Response to Vibration and Acoustic Excitation," Northrop Corporation, NOR 66-64, NASA Contract NAS8-11360, Jan. 1966.

[3] Ballentine, J.R. et al., "Refinement of Sonic Fatigue Structural Design Criteria," Air Force Flight Dynamics Laboratory, AFFDL-TR-67-156, Jan. 1968.

[4] Rudder, F.F. Jr., "Acoustic Fatigue of Aircraft Structural Component Assemblies," Air Force Flight Dynamics Laboratory, AFFDL-TR-71-107, Feb. 1972.

[5] Jacobson, M.J., "Sonic Fatigue Design Data for Bonded Aluminum Aircraft Structures," Air Force Flight Dynamics Laboratory, AFFDL-TR-77-45, June 1977.

[6] Jacobson, M.J., "Acoustic Fatigue Design Information for Fiber-Reinforced Structures," Air Force Flight Dynamics Laboratory, AFFDL-TR-68-107, Oct. 1968.

[7] Jacobson, M.J., "Advanced Composite Joints; Design and Acoustic Fatigue Characteristics," Air Force Flight Dynamics Laboratory, AFFDL-TR-71-126, April 1972.

[8] Holehouse, I., "Sonic Fatigue Design Techniques for Advanced Composite Aircraft Structures," Air Force Wright Aeronautical Laboratory, AFWAL-TR-80-3019, April 1980.

[9] Jacobson, M.J., "Effect of Structural Heating on the Sonic Fatigue of Aerospace Vehicle Structures," Air Force Flight Dynamics Laboratory, AFFDL-TR-73-56, Jan. 1974.

[10] Schneider, C.W., "Acoustic Fatigue of Aircraft Structures at Elevated Temperatures," Air Force Flight Dynamics Laboratory, AFFDL-TR-73-155, Parts I and II, 1974.

[11] Rudder, F.F. Jr. and Plumblee, H.E. Jr., "Sonic Fatigue Design Guide for Military Aircraft," Air Force Flight Dynamics Laboratory, AFFDL-TR-74-112, May 1975.

[12] Jacobson, M.J., "Fatigue of V/STOL Composite Fuselage Panels Under Acoustic-Thermal Environments," Naval Air Development Center, NADC-81045-60, March 1981.